PROPOSAL

Measurement of G_{Ep}/G_{Mp} to Q^2=9 GeV^2 Via recoil polarization

C.F. Perdrisat (co-spokesperson), T. Averett, O. Gayou[†]
College of William and Mary

Vina Punjabi (co-spokesperson), C. Salgado
Norfolk State University

M.K. Jones (co-spokesperson) C. C. Chang, J. Kelly
University of Maryland

E. Brash (co-spokesperson), G. Huber, A. Kozlov, G. Lolos, Z. Papandreou
University of Regina, Canada

M. Epstein, D. Margaziotis
California State University at Los Angeles

E. Tomasi-Gustafsson
DAPNIA, Saclay, France

C. Howell, S. Churchwell
Duke University/TUNL

B. Milbrath
Eastern Kentucky University

R. Carlini, E. Chudakov, R. Ent, K. Garrow, J. Gomez, N. Liyanage, J. Mitchell, D. Mack, D. Meekins, W. Vulcan, B. Wojtsekhowski
Jefferson Lab

W. Boeglin, P. Markowitz, B. Raue, J. Reinhold
Florida International University and Jefferson Lab

K. Baker, C. Keppel
Hampton University

A. Nathan, K. Wijesooriya
University of Illinois

L. Bimbot
Institut de Physique Nucléaire, Orsay, France

N. Merenkov
Institute of Physics and Technology, Kharkov, Ukraine

G. Quéméner
Institut des Sciences Nucléaires, Grenoble, France

V.P. Kubarovsky, Yu.M. Goncharenko, A.P. Meschanin, L.F. Soloviev and A.N. Vasiliev
Institut for High Energy Physics, Protvino, Russia

E. Cisbani, S. Frullani, F. Garibaldi, R. Iommi
INFN-ISS, Italy

M. Iodice
INFN-Roma3, Italy

G.M. Urcioli
INFN Roma1, Italy

R. de Leo
INFN Bari, Italy

K. Fissum
University of Lund, Sweden

N. Piskunov, D. Kirillov, I. Sitnik, Yu. Zanesvky
Laboratory for High Energy, JINR, Dubna, Russia

W. Bertozzi, D. Higinbotham, S. Gilad, S. Sirca, R. Suleiman, Z. Zhou
Massachussetts Institute of Technology

M. Rekalo
Middle East Technical University, Turkey

J. Calarco
University of New Hampshire

B. Vlahovic, A. Afanasev and I. Akushevich
North Carolina Central University

A. Radyushkin, P. Ulmer
Old Dominion University

S. Dieterich, R. Gilman, C. Glashausser, X. Jiang, G. Kumbartzki, R. Ransome and S. Strauch
Rutgers University

H. Voskanian, K. Egiyan, A. Ketikyan
Yerevan Physics Institute, Armenia

* The name of collaborators assuming responsibility for development of a part of the instrumentation are underlined.
† also Université Blaise Pascal, Clermont-Ferand,France

Abstract

We propose to measure the ratio of electromagnetic form factors of the proton, G_{Ep}/G_{Mp}, to Q^2=9 GeV^2 in elastic electron scattering from hydrogen in Hall C with the recoil polarization technique. The proton will be detected in the HMS and the electron in a large solid angle lead glass calorimeter. This experiment is an extension of experiment 99-007 which will measure G_{Ep}/G_{Mp} up to Q^2=5.6 GeV^2 later this year in Hall A. The data from JLab experiment 93-027 have shown an unexpected and significant difference between the electric and magnetic form factors, starting at Q^2=1 GeV^2, up to the maximum value of 3.5 GeV^2, revealing a different spatial distribution for charge and magnetization. These data also clearly demonstrated that we have not yet reached the perturbative QCD limit, which would be signaled by the ratio Q^2F_{2p}/F_{1p} becoming constant.

The proposed data, together with the existing G_{Mp}-data, will determine both F_{1p} and F_{2p}, the Dirac and Pauli form factors, separately. At large Q^2, F_{1p} is already well determined from existing G_{Mp} data. This experiment will extend the knowledge of F_{2p}, which is equally sensitive to G_{Ep} and G_{Mp} , to a Q^2 region where, in the pQCD picture, helicity conservation should operate. For each one of these reasons, measurement of G_{Ep}/G_{Mp} up to 9 GeV^2 is of great interest. This Q^2 region is thought to be the one of transition between soft and hard scattering, and is the most challenging theoretically. Ultimately, understanding of this difficult region will be achieved from QCD, the theory of the strong interaction. The data from this experiment will provide a testing ground for theory.

This experiment requires 6 GeV incident electron energy, and thus is possible before the anticipated energy upgrade of the CEBAF accelerator.

1 Introduction

Experiment 93-027 in Hall A measured G_{Ep}/G_{Mp}, with an precision comparable to that of G_{Mp}, to Q^2=3.5 GeV^2. The now published[1] results of 93-027 are shown in Fig. 1; displayed on the left of Fig. 1 are the ratios G_{Ep}/G_D obtained from the 93-027 results, together with the world data, and the G_{Mp} world data are shown on the right. The most important feature of the new JLab data is the sharp decline of the ratio G_{Ep}/G_D as Q^2 increases, which indicates that G_{Ep} falls faster than G_{Mp}. Hence the new JLab data has demonstrated a significant difference in the Q^2-dependence of the elastic electric and magnetic form factors of the proton starting at 1 GeV^2. These new data for G_{Ep} have created much excitement in the Nuclear Physics community, and the most important question raised by these results is whether G_{Ep} will continue to decrease with increasing Q^2.

PAC 15 approved proposal 99-007, to extend the measurement of the G_{Ep}/G_{Mp}-ratio to Q^2=5.6 GeV^2 in Hall A. This has become possible now at JLab, in part because of the greatly improved beam performance, both in polarization and intensity, and in part by replacing the present 50 cm thick graphite analyzer in the hadron HRS focal plane polarimeter (FPP) , with 100 cm of CH_2. Experiment 99-007 is scheduled to run in Hall A in November-December 2000.

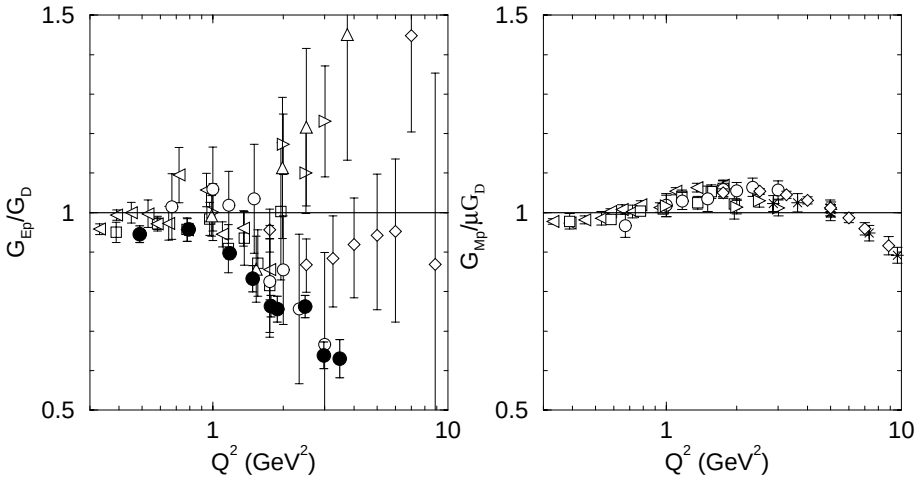

Figure 1: The published results of experiment 93027 presented as the ratio G_{Ep}/G_D and compared to the previous world results (Refs. [2],[3],[4], [5],[6], [7], [8], and [9]). On the right is the ratio $G_{Mp}/\mu_p G_D$, where $G_D = (1 + \frac{Q^2}{0.71})^2$. This highlights the dramatically different Q^2 dependence of the two form factors.

In this proposal we show that it is now possible to extend the measurement of the G_{Ep}/G_{Mp} ratio to yet larger Q^2 values at JLab in Hall C; there is no other accelerator and detector facility in the world where such measurements could be made. We will show here that by installing a new focal-plane polarimeter (FPP) in the detector hut of the HMS in Hall C, with 120 cm of CH_2, and a large area lead-glass calorimeter to detect the electron, we can extend these measurements to a Q^2 of 9 GeV^2. The absolute uncertainties on these new data will be less than 0.07. The beam energy required is 6 GeV.

The characterization of the structure of the nucleon is the defining problem of hadronic physics, as the hydrogen atom is to atomic physics. Elastic nucleon form factors are key ingredients of this characterization. Ideally all four elastic nucleon form factors should be measured to the highest possible Q^2. Currently only G_{Mp} is known up to about Q^2 of 15 GeV^2 with an accuracy better than 5% and to 31 GeV^2 with an uncertainty of $\sim 10\%$. New measurements of G_{Mn} in Hall B[11] are currently being analyzed; they will bring the knowledge of this form factor to comparable levels of accuracy up to Q^2=7.5 GeV^2. For the neutron electric form factor, new experiments at JLab[12] will reach Q^2=1.48 GeV^2 with an accuracy comparable to the 3 other form factors.

The experiment proposed here would extend the range over which G_{Ep} is well defined to Q^2 of 9 GeV^2. In the future, it might become possible to extend the Q^2 range of G_{Ep} and G_{Mn} to approximately 14 GeV^2 with 12 GeV polarized beams at JLab.

2 Theoretical Interest

In electron scattering at high Q^2, the dominant degrees of freedom in the nucleon are the three valence quarks. This is the regime where perturbative QCD theory can be applied[10]. At $Q^2 < 1$ GeV^2, the Vector Meson Dominance (VMD) model[13, 14, 15] has been successful in describing the nucleon form factors and hadronic interactions. Predicting nucleon form factors in the transition region between low Q^2, where the meson picture is valid, and the high Q^2 region where pQCD is valid, is very difficult. There is also a great deal of controversy over where the pQCD approach becomes applicable. There are many theoretical approaches to calculate the elastic nucleon form factors, and some of them are: the relativistic constituent quark model (RCQ)[16, 17, 18], the di-quark model[19], sum rules[20], and the cloudy bag model[21], to name a few. In fact, the form factors are in many senses the most fundamental observables of these theories. Hence, precise measurements of hadronic form factors serve as a crucial test for the theories, which must be passed before extending to other reactions such as meson photo- and electro-production, real Compton scattering, or deuteron photo-disintegration.

We can gain some insight into why the elastic nucleon form factors represent such an important first comparison point for the theories by considering the helicity conserving Dirac form factor, F_{1p}, and the helicity non-conserving Pauli form factor, F_{2p}. The Sachs form factors, G_{Ep} and G_{Mp}, are related to F_{1p} and

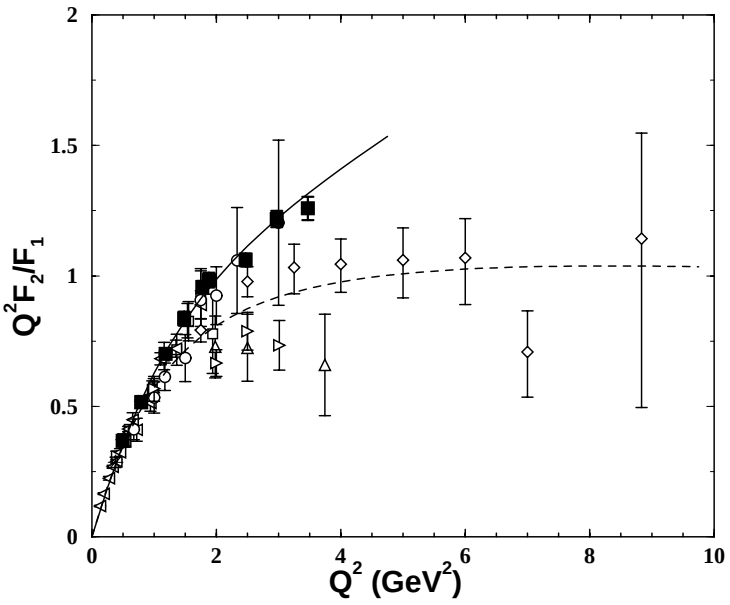

Figure 2: The dashed line is obtained using $G_{Ep} = G_D$. The solid line is a fit to the E93027 data, and is meant as a guide to the eye. The symbols are the same as in Fig.1.

F_{2p}, by the following equations:

$$F_{1p} = \frac{G_{Ep} + \tau G_{Mp}}{1+\tau} \text{ and } F_{2p} = \frac{G_{Mp} - G_{Ep}}{\kappa(1+\tau)} \quad (1)$$

The Dirac and Pauli form factors, from the standpoint of comparison to theory, are fundamental. The Vector Meson Dominance model, which is valid at low Q^2, and pQCD, which must be valid at large Q^2, predict very specific, yet very different, Q^2-dependencies for both F_{1p} and F_{2p}. Thus, understanding the Q^2 evolution of these form factors allows us to map the transition from the soft to the hard scattering regimes.

To illustrate this point, we note that in the pQCD approach, F_{1p} has a Q^{-4} dependence and F_{2p} has a Q^{-6} dependence. It is therefore a prediction of pQCD that $Q^2\ F_{2p}/F_{1p}$ should become constant for large Q^2 as demonstrated long ago by Brodsky and Lepage[10]. Moreover, these authors point out that a detailed understanding of the Q^2 evolution of the form factors in the Q^2-range of this experiment, is a crucial ingredient in this theory, especially since the overall normalization is not fixed.

In Fig. 2, we show Q^2F_{2p}/F_{1p} extracted directly from the JLab data of experiment 93-027, and the previous world data. What appeared to be an early flattening of the Q^2F_{2p}/F_{1p} ratio to a constant value is not confirmed by the JLab data. Next we look at the Q^2 dependence of F_{1p} and F_{2p} separately.

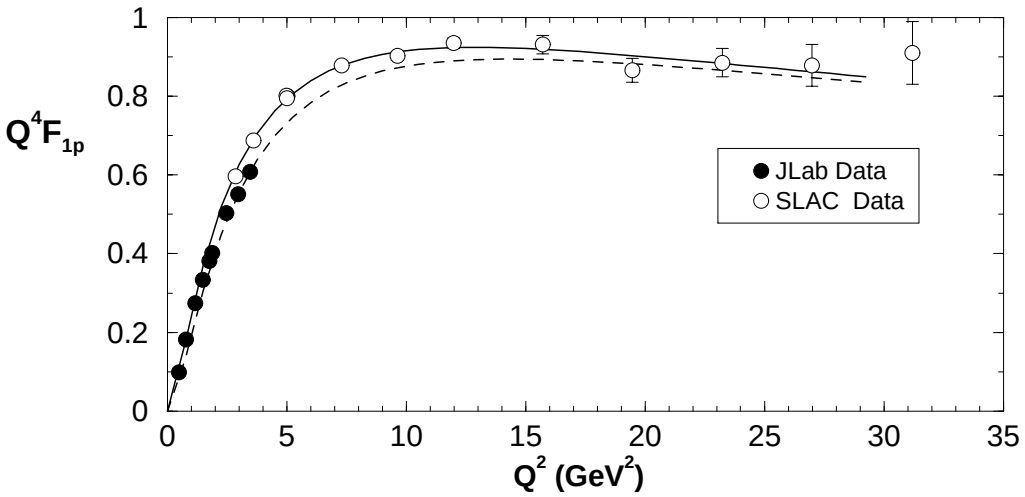

Figure 3: The solid points are Q^4F_{1p} calculated using G_{Ep}/G_{Mp} of 93-027 and G_{Mp} from the Bosted fit to world data. The open points are from Ref. [9] which assumed $\mu G_{Ep}/G_{Mp} = 1$ in calculating F_{1p} from their measured G_{Mp} data.

In the paper of Sill et al.[9], G_{Mp} was determined to $Q^2 \approx 30$ GeV^2 by measuring elastic ep cross sections and assuming $\mu G_{Ep}/G_{Mp} = 1$. The Q^4F_{1p} values extracted from these data, again assuming $\mu G_{Ep}/G_{Mp} = 1$, are plotted in Fig. 3. As seen in this figure, Q^4F_{1p} starts flattening out at ~ 9 GeV^2, and this has been interpreted as an indication of the onset of pQCD. Given that the new JLab data increasingly differ from 1 as Q^2 increases, one may wonder what effect this has on Q^4F_{1p}. The difference is illustrated in Fig.3 where the solid line corresponds to the assumption $\mu G_{Ep}/G_{Mp}$=1 and the dotted line to the ratio $\mu G_{Ep}/G_{Mp}$=0.61, the value obtained at Q^2=3.5 in ref.[1]. This figure illustrates the insensitivity of Q^4F_{1p} to G_{Ep}; it is of course a consequence of Eq. 1, because of the factor of τ in front of G_{Mp}.

In contrast to F_{1p}, F_{2p} is very sensitive to G_{Ep}. If one assumes $\mu G_{Ep}/G_{Mp} = 1$ at all Q^2, then the contribution of $\mu G_{Ep}/G_{Mp}$ to F_{2p} is 55% at all Q^2. In Fig. 4, we show the values of Q^6F_{2p} obtained by combining the new JLab G_{Ep}/G_{Mp} data with G_{Mp} values from the Bosted[22] fit to the world data. The solid line in Fig. 4 is the prediction of Q^6F_{2p} assuming $\mu G_{Ep}/G_{Mp} = 1$, and the dotted line is for $\mu G_{Ep}/G_{Mp}$ =0.62. As seen in this figure, the difference between the two predictions increases with Q^2; it would further increases if the G_{Ep}/G_{Mp} was to further decreases from the 0.61 value. Of course, the critical question is: what will be the Q^2 dependence of F_{2p} in the Q^2 range of this proposal, in particular will it reach a constant value? The answer to this question can only be supplied by data, and therefore the data from this experiment will have a very significant impact on the theory of the nucleon.

In a more general framework, the asymptotic behavior of both space-like

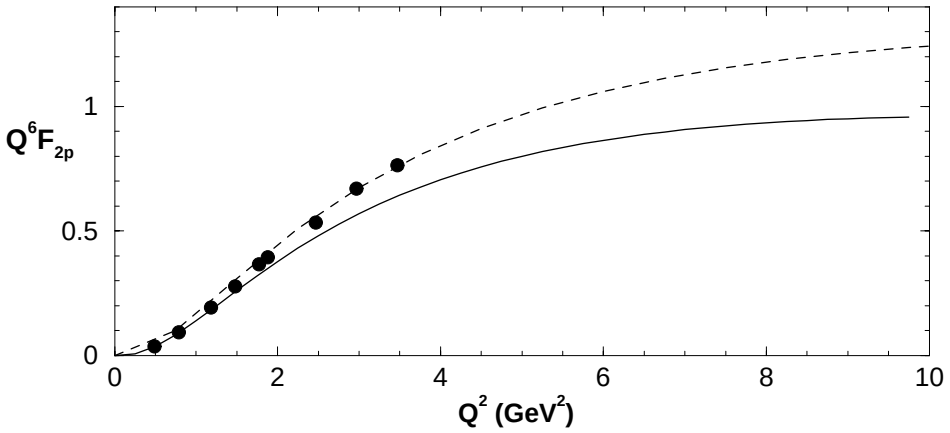

Figure 4: The solid points are Q^6F_{2p} calculated using G_{Ep}/G_{Mp} of 93-027 and G_{Mp} from the Bosted fit to world data.

and time-like elastic form factors are connected. Application of the Phragmén-Lindelhöf theorem[23] to the form factors shows that their asymptotic behavior must be the same, and that their ratio should go to 1 as $Q^2 \to \infty$. The existing time-like proton form-factor data show that this condition is far from being satisfied at Q^2=13 GeV^2. The possibility that the present data can be entirely understood from soft contributions had already been pointed out by Nesterenko and Radyushkin[24], and discussed by Isgur and Llewellyn Smith[25].

Recent theoretical developments indicate that measurements of the separated elastic form factors of the proton to large Q^2 may shed light on the problem of nucleon spin. This connection between elastic form factors and spin has been demonstrated within the formalism of Generalized Parton Distributions (GPD). The first moment of the GPD taken in the forward limit yields, according to the Angular Momentum Sum Rule[26], a contribution to the nucleon spin from the quarks and gluons, including the orbital angular momentum. The t-dependence of GPD's has been modeled using a factor corresponding to the relativistic Gaussian dependence of both Dirac[27] and Pauli[28] form factors of the proton. Extrapolation of these GPD's to t=0 leads to the functions entering into the Angular Momentum Sum Rule, and an estimate of the contribution of the valence quarks to the proton spin can then be obtained. This approach was used recently by Afanasev[29] who, using the G_{Ep}/G_{Mp} data of experiment 93-027 in the framework of GPD, concluded that valence quarks contribute about 50% to the nucleon spin. When combined with semi-exclusive data from SMC[30], this result implies that about 25% of the proton spin comes from the orbital angular momentum of the valence quarks.

There are also lattice QCD calculations predicting the contribution to the proton spin coming from angular momentum of the valence quarks. For example, Mathur et al.[31] calculate the quark orbital angular momentum of the proton

from the quark energy-momentum tensor form factors on the lattice. They calculate the total contribution from the quarks to be 60%, and hence 35% of the proton spin originates from the orbital angular momentum. These calculations are performed in a rigorous and gauge invariant formalism, and the general agreement with the GPD calculation of Afanasev is encouraging.

An extension of the measurements of the G_{Ep}/G_{Mp} ratio to higher momentum transfers will constrain the x-dependence of the GPD and represent a major step towards a characterization of the quark spin and orbital angular momentum contributions to the proton spin.

3 The Recoil Polarization Method

In experiment 93-027 we used the recoil polarization method successfully to measure the ratio G_{Ep}/G_{Mp} up to Q^2 =3.5 GeV^2. In November-December 2000 experiment 99-007 will measure the ratio G_{Ep}/G_{Mp} up to $Q^2 = 5.6$ GeV^2 using the same polarization technique. Here, we are proposing to use this technique to measure the G_{Ep}/G_{Mp}-ratio to $Q^2 = 9.0$ GeV^2.

The polarization method was first discussed by Akhiezer and Rekalo[32] and later by Arnold, Carlson and Gross [33]. With longitudinally polarized electrons one can either use a polarized target, or measure the transferred longitudinal and sideways polarizations, P_ℓ and P_t, respectively, of the recoiling proton with a polarimeter. Starting above 1 GeV^2, this technique is superior to the traditional Rosenbluth separation technique. The first advantage of the polarization method is that it requires no change of energy or angle. For each Q^2 a single measurement of the azimuthal distribution of the protons diffused in a secondary scatterer determines simultaneously both P_ℓ and P_t.

As given in ref.[33], for one photon exchange, P_ℓ and P_t are:

$$I_0 P_l = \frac{1}{M}(E_e + E_{e'})\sqrt{\tau(1+\tau)}G_{Mp}^2 \tan^2\frac{\theta_e}{2} \quad (2)$$

$$I_0 P_t = -2\sqrt{\tau(1+\tau)}G_{Ep}G_{Mp}\tan\frac{\theta_e}{2} \quad (3)$$

where

$$I_0 = G_{Ep}^2(Q^2) + \tau G_{Mp}^2(Q^2)[1 + 2(1+\tau)\tan^2\frac{\theta_e}{2}] \quad (4)$$

The second advantage of the polarization method is that the relevant observable, P_t, (see Equ.3 is an interference term; thus even a small G_{Ep} will get amplified by the large G_{Mp}.

With a focal plane polarimeter, one measures the azimuthal angular distribution after a second scattering in an analyzer. This distribution has two components only, corresponding to the two projections of the polarization in the plane of the analyzer. The azimuthal distribution measured in a polarimeter with an azimuthal angle acceptance of 2π can be written as:

$$N_p(\theta,\varphi) = N_p(h=0)\epsilon(\theta)(1 \pm |h| A_c(\theta)[P_{t'}\sin\varphi - P_{n'}\cos\varphi]) \tag{5}$$

where h is the electron beam polarization, and the $\pm$ stands for the two possible orientations of the electron longitudinal polarization, N_p(h=0) is the number of protons incident on the polarimeter, θ and φ are the polar and azimuthal angles after scattering in the analyzer, $\epsilon(\theta)$ is the differential efficiency, and $A_c(\theta)$ the analyzing power of the analyzer, $P_{t'}$ and $P_{n'}$ are the transverse and normal, in-plane components, of the polarization at the analyzer.

For a spectrometer consisting of a single dipole with homogeneous field, the spin transport matrix connecting the polarizations at the analyzer and at the target reduces to:

$$\begin{pmatrix} P_{n'} \\ P_{t'} \\ P_{\ell'} \end{pmatrix}_{fp} = \begin{pmatrix} \cos\chi & 0 & \sin\chi \\ 0 & 1 & 0 \\ -\sin\chi & 0 & \cos\chi \end{pmatrix} \begin{pmatrix} P_n \\ P_t \\ P_\ell \end{pmatrix}_{tgt}$$

where χ is the spin precession angle in the spectrometer.

In the case of elastic ep scattering, P_n=0 in the single photon exchange approximation. Thus, in this case, in the single dipole approximation the relationships between target and focal plane components are:

$$P_{t'} = P_t \text{ and } P_{n'} = P_\ell \sin\chi \tag{6}$$

The Fourier analysis of the experimental azimuthal distribution $N_p(\theta,\varphi)$ in Equ.5, together with Equ.6, gives the two physical amplitudes for each bin of θ in terms of the polarization components at the target:

$$a(\theta) = hA_c(\theta)P_t \text{ and } b(\theta) = hA_c(\theta)P_\ell \sin\chi \tag{7}$$

from which P_t and P_ℓ can be obtained.

In a spectrometer with quadrupoles and shaped dipole(s) further spin rotation occurs in these higher order magnetic fields (quadrupole, sextupoles...). Therefore, the actual spin transfer matrix ($S_{n'm}$) has nine non-zero matrix elements. These matrix elements are different for every event, because they depend on $(\theta, y, \varphi, \delta)_{tgt}$. To extract the physical quantities P_t and P_ℓ one must correct for spin precession for each event. The method we have been using in the analysis is directly based on the Fourier analysis. One can show that the quantities a(θ) and b(θ) in Eq. 7 are the sums over all events in the azimuthal distribution, as follows:

$$a(\theta) = \frac{2}{N}[\sum_i^N (S^{(i)}_{n't} hA_c(\theta)P_t \cos^2\varphi_i + S^{(i)}_{n'\ell} hA_c(\theta)P_\ell cos^2\varphi_i)] \tag{8}$$

$$b(\theta) = \frac{2}{N}[\sum_i^N (S^{(i)}_{t't} hA_c(\theta)P_t sin^2\varphi_i + S^{(i)}_{t'\ell} hA_c(\theta)P_\ell \sin^2\varphi_i)] \tag{9}$$

where index i numbers the events. These equations can be solved for the 2 unknowns $(hA_c(\theta)P_t)$ and $(hA_c(\theta)P_\ell)$. The $S_{n'm}$ matrix elements have to be calculated from a model of the spectrometer. The spectrometer will be modeled with COSY, a differential algebraic code.

The ratio G_{Ep}/G_{Mp} can then be obtained directly from the ratio $r(\theta)=\frac{hA_c(\theta)P_t}{hA_c(\theta)P_\ell}$:

$$G_{Ep}/G_{Mp} = -r(\theta)\frac{(E_e + E_{e'})}{2M}\tan(\frac{\theta_e}{2}) \tag{10}$$

The definition of P_t and P_ℓ (Eqns. 2 and 3) can then be used to calculate these two components from the measured G_{Ep}/G_{Mp} leading to a calculation of the quantity $hA_c(\theta)$. The beam polarization will be measured independently with the Møller polarimeter in Hall C, thus providing a calibration of the polarimeter analyzing power for each of the proton energies of this proposal.

4 Experimental considerations

4.1 Introduction

This experiment will use the High Momentum Spectrometer (HMS) in Hall C to detect the recoiling proton, and the scattered electron will be detected in a calorimeter, a large solid angle detector. The focal plane in the HMS will be equipped with a polarimeter to measure the polarization of the recoil proton. Following subsections describe the modifications and additions to existing equipment in Hall C necessary to carry out this experiment.

4.1.1 The High Momentum Spectrometer

The HMS bends charged particles in the vertical plane; it consists of 3 quadrupoles followed by one dipole. Its angular acceptance is 60x130 mr^2 in the horizontal and vertical direction, respectively. The angular resolution is 1 mr and the momentum resolution is $< 10^{-3}$. The momentum and angular resolutions are perfectly adequate for this experiment. The highest momentum accepted by the HMS is 7.5 GeV/c, corresponding to Q^2=12.4 GeV^2, and the bend angle of the HMS is 25°.

As described in the previous section, favorable precession angles are crucial to obtain the ratio G_{Ep}/G_{Mp} with small uncertainty. In this experiment we will extract P_t and P_ℓ at the target from the measured quantities $P_{t'}$ and $P_{n'}$ at the analyzer; equation (6) makes it clear that $sin\chi$=0 must be avoided, otherwise $P_{n'}$=0. The precession angles corresponding to the Q^2 values proposed here, 6.5, 7.5 and 9 GeV^2, are between 210 to 274°; all 3 angles are very favorable and actually the one corresponding to 9 GeV^2 is the best possible.

4.1.2 The Focal Plane Polarimeter

This experiment requires the installation of a new polarimeter in the focal plane area of the HMS, following the scintillators S1X and S1Y. As shown in Fig. 5, the analyzer is divided into two blocks, each 60 cm thick. The incoming proton trajectories will be reconstructed from the existing HMS focal plane drift chambers DC1 and DC2. An (xy) drift chamber with good angular resolution will follow each CH_2 block to reconstruct the trajectory after the scattering in the analyzer. There are at least two advantages to this configuration: first the chamber dimensions are minimized, and second, events with one nuclear scattering in either one of the blocks can be identified and analyzed separately.

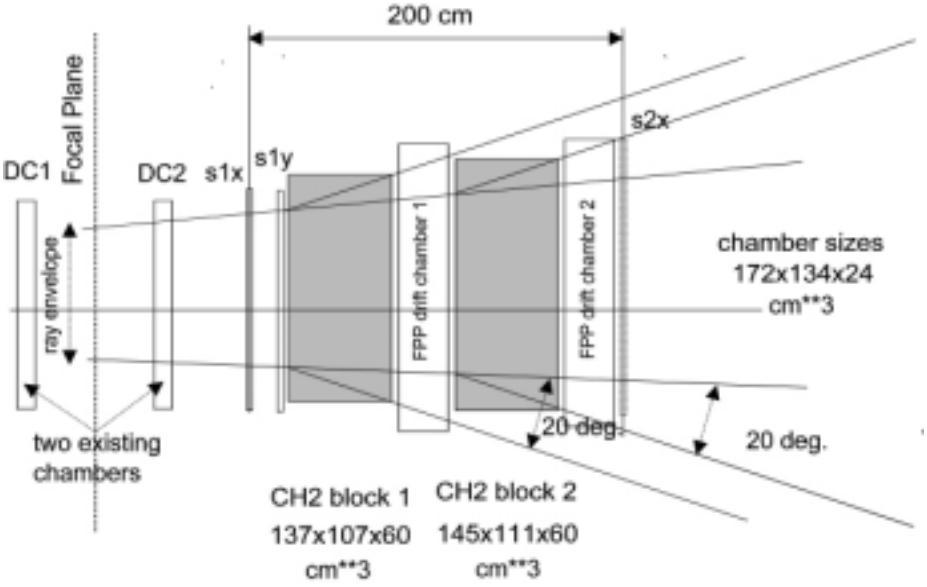

Figure 5: Sideview to scale, of the planned new polarimeter for the HMS (in the dispersive direction); S1 and S2 are the scintillator planes which will define the trigger.

The crucial feature of the polarimeter is its figure of merit (FOM), defined as FOM=ϵA_y^2, where ϵ is the usable fraction of events scattered in the analyzer, and A_y^2 is the weighted average of the analyzing power squared. As presented in the 99-007 proposal for Hall A, adding hydrogen to the analyzer increases its FOM because the analyzing power in pp scattering is becoming increasingly better than that of the graphite, for increasing proton energy. As seen in Fig.6 the pC analyzing power decreases rapidly with increasing proton energy. In this figure the data are from experiment 93-027. The solid lines represent the fits used as input to the GEANT Monte Carlo simulation[34] done to prepare this experiment. Similar fits have been carried out for the currently available pC and pp scattering data. The average analyzing powers for pC and pp calculated

with this Monte Carlo simulation, are shown in Fig. 7; for example at T_p=3.2 GeV, the ratio of the pp to pC analyzing powers is ∼3; this ratio increases as the proton energy increases. Currently, the highest proton energy for which we have graphite analyzing power data is 3.61 GeV [35]; for pp scattering it is 10 GeV/c[36].

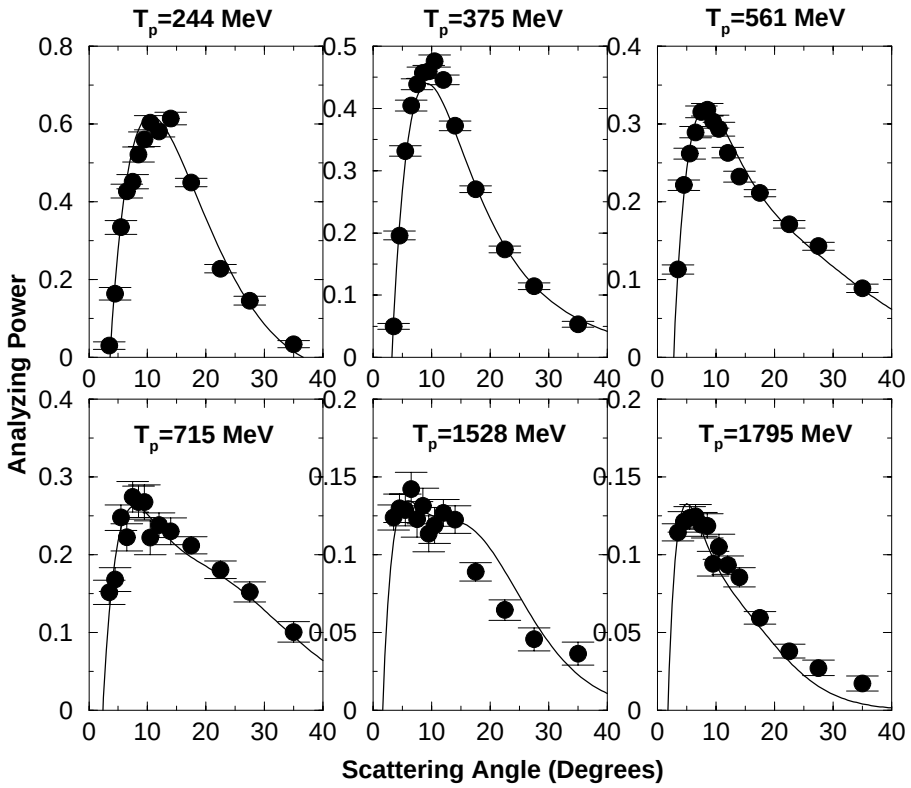

Figure 6: The carbon analyzing power extract from the data of experiment 93-027, together with the fits (solid line) used as input to the Monte Carlo simulation.

The FOM values calculated with the Monte Carlo simulation for the new polarimeter are given in table 1; this simulation also indicates that the optimum thickness of CH_2 is 60 to 80 cm. The design of the FPP takes this fact into account: it consists of two independent polarimeters in series, each with optimum thickness, with the possibility to eliminate their interference.

The two new chambers required for this polarimeter will be identical; their sensitive area will be of $\sim 172 \times 134$ cm^2. These chambers must have an angular resolutions of about 1 mr (1σ); drift chambers will satisfy this requirement. We have a preliminary estimate of time and cost to build these chambers from the Technical Services of DAPNIA, Saclay. We have also discussed their con-

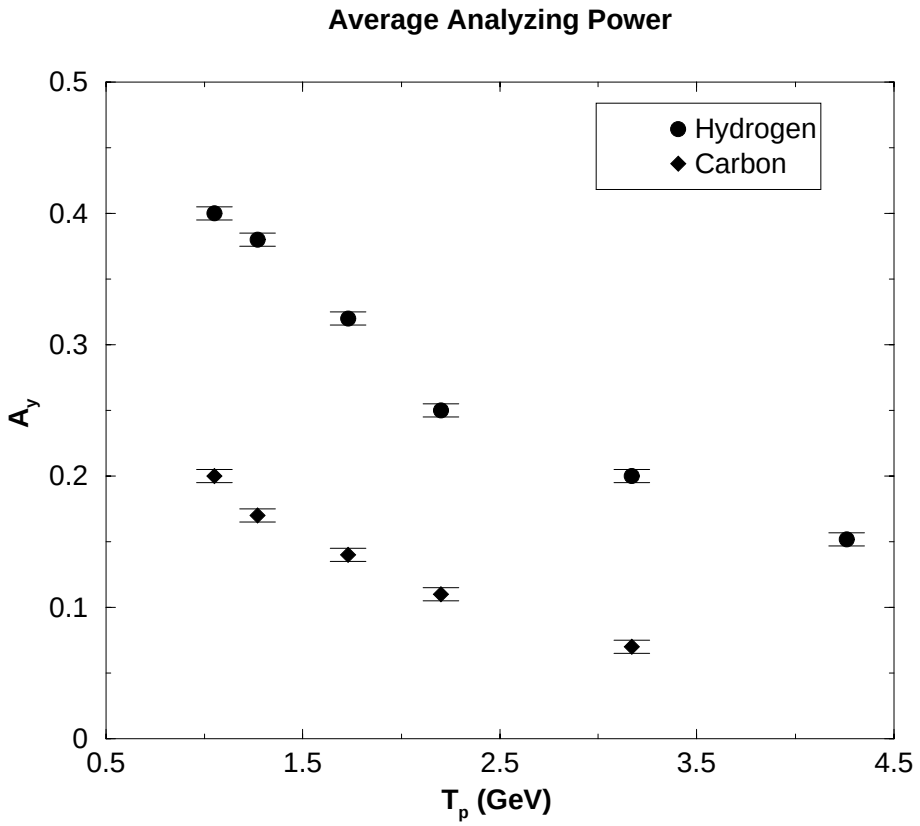

Figure 7: The Monte Carlo results for the analyzing power in pC and pp; the angular averaging is over 5 to 20°..

struction with the Detector Group at LHE, Dubna. Both groups have much experience with the fabrication of large drift chambers. The co-PI's will coordinate the design, construction and installation of the FPP. The FPP will be designed as a unit in a sturdy frame, to facilitate its installation and removal. Once the polarimeter is installed in the HMS focal plane, it may remain a part of its instrumentation, interchangeable with the gas Cerenkov.

4.1.3 The Calorimeter

Essential to this experiment is solid angle matching. With the accelerator energy limited to 6 GeV, all the kinematics of this proposal have an electron scattering angle larger than the proton recoil angle; therefore the Jacobian for the electron is larger than 1, and hence the solid angle for the electron detector must be larger than that of the proton detector if all elastic ep events are to be captured. In

this experiment protons will be detected in the HMS. To fully utilize the HMS solid angle, the electron must be detected in a device with larger solid angle than the HMS. Based on the design and tests for the Real Compton Scattering experiment in Hall A [37], we have adopted the technique of using a calorimeter made of lead-glass blocks to detect the electron. This well understood technique will provide an angular resolution comparable to that of the HMS. The idea is to separate elastic ep scattering by selecting events with angles satisfying the 2-body kinematics; the better the angular resolution, the better the separation. The TDC information from each lead-glass block will be used to eliminate most of the accidental events. Our studies in Hall A, to be described below, indicate that the target walls contribution is negligible. The great advantage of Cerenkov lead-glass detector is their relative insensitivity to pions and low energy particles.

The feasibility of this technique was investigated in two test runs in Hall A this Spring. In both test runs we used a prototype calorimeter with a 5 (horizontal)$\times$9(vertical) array of 15$\times$15 cm^2 lead glass blocks; the position resolution of the detector is approximately $15/\sqrt{12}$=4.3 cm (1σ) when the position is defined by one block only; for about 30% of the events a better resolution was obtained using the energy deposited in a neighbor block to calculate the position of the scattered electron.

In the first test the beam energy was 3.08 GeV and two elastic ep kinematics were chosen, Q^2=2.5 and 3.5 GeV^2. For the latter, the calorimeter was at 58^0 to the beam, 5.45 m away from the target, giving a single-hit angular resolution of 8 mr (1σ); the HRS in Hall A detected the associated proton at 23^0.

In the second test in May 2000 the energy was 3.395 GeV, the calorimeter was at an angle of 41° and at a distance of 8 m. In this test we collected data for background studies with empty target cell and no cell to determine what part of the background comes from the target walls, and what part from the environment (beam dump). We also measured accidentals by delaying the ADC gate and, to evaluate the usefulness of TOF information, we connected two of the lead-glass blocks to TDC's. In this test we also re-measured the G_{Ep}/G_{Mp} ratio of experiment 93-027 at Q^2=3.0 GeV^2; the preliminary results obtained in 21 hours of beam on target ($\sim$50 μA, beam polarization 71.2%) are $\mu_p G_{Ep}/G_{Mp}$= 0.62$\pm$0.048, to be compared with the published results 0.61$\pm$0.032; the uncertainties given are statistical only. These results were obtained without using any TDC information from the calorimeter.

Some of the results of the preliminary analysis of this test are shown in Fig 8. The top left shows the raw ADC spectrum in one block; the elastic events are in the peak at 1800 MeV ; next is the corresponding TDC spectrum, with a sharp elastic peak. To the right then is the ADC spectrum conditioned by an appropriate TDC cut. The tail on the left is part radiative tail, and part spilling over from showers in a neighboring block.

The middle row shows the missing energy spectrum for all events, $E_{miss} = E_{beam} - E_p - E_e$. Next is the same spectrum, conditioned by a cut on the elastic peak in the HRS focal plane. On the right is the result with an additional cut on θ_e-θ_p and ϕ_e- ϕ_p correlation. The remaining events are the elastic ep ones only.

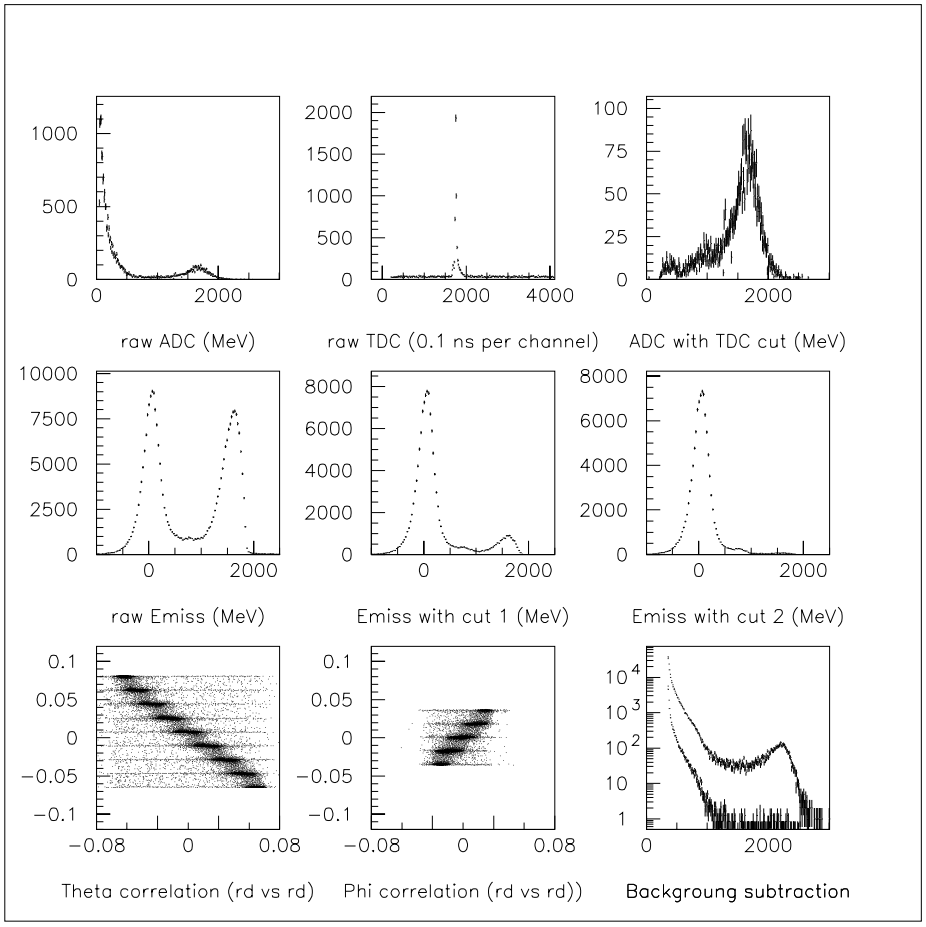

Figure 8: From left to right, top to bottom:
raw ADC spectrum for 1 lead-glass block
raw TDC spectrum for the same block
same ADC spectrum after cut on elastic peak in TDC
E_{miss}-spectrum for all events, no cut. The elastic events are in the peak at $E_{miss} = 0$
E_{miss} after cut on the elastic peak in the HRS focal plane (not shown here).
E_{miss} with additional cut on the θ and ϕ ep angular correlation; the elastic peak now stands alone
θ_e- θ_p angular correlation, all events
ϕ_e- ϕ_p angular correlation, all events
raw ADC spectrum, real and empty target for one block

The lower row shows the θ_e-θ_p and ϕ_e- ϕ_p correlations in the first two panels. The last panel shows again an ADC spectrum, all events, and the empty target events, normalized. The accidental events would be eliminated by a cut on the TDC peak. The empty target contribution under the elastic peak is about 10^{-4}.

The conclusion of the test is that this method is viable, and if the angular resolution is sufficient then, the elastic events can be fully separated from the background events. We anticipate larger background for the proposed experiment in hall C. However, as explained above, using the TDC information will reject most of the HMS-calorimeter accidentals. With a calorimeter angular resolution matching that of the HMS, $\sim$2 mr, we expect to achieve full separation of elastic events up to the largest Q^2- value proposed here. In fact the cross section at Q^2=5.6 GeV^2 is only 10 times smaller than the cross section at Q^2=3.0 GeV^2 under the condition of the test. The target empty rate is then going to be at the most 10^{-3} of the elastic ep rate.

The largest solid angle required in this experiment is 135 msr, at Q^2 of 9 Gev^2; for this Q^2 the calorimeter will be located at 68° and a distance of 4.35 m from the target. To obtain the desired solid angle we are planning to assemble a large calorimeter with 1600 4x4 cm^2 lead-glass blocks, each connected to an ADC and a TDC. The expected position resolution is 3-5 mm, which will translate into an angular resolution of 1-2 mr. The accidentals will be eliminated from cuts on the TDC information from each lead-glass block. It will be necessary to shield the calorimeter from neutrons generated in the beam dump and to build a platform for the calorimeter.

The primary responsibility for the calorimeter of this experiment will be with B. Wojtsekhowski (JLab, Hall A), H. Voskanyan (Yerevan) and V.P Kubarovsky (Protvino).

5 The proposed measurements

Here we propose to measure the G_{Ep}/G_{Mp}-ratio for 3 new values of Q^2: 6.5, 7.5 and 9 GeV^2, and a control point at 4.2 GeV^2 which coincides with one of 99-007.

The largest Q^2 we can measure in a reasonable time in Hall C, given the limitation of a 6 GeV beam, is 9 GeV^2, which can be determined by looking at the statistical uncertainty achievable in a given time for specified current and beam polarization. This is illustrated in Fig. 9, which clearly shows that with a 6 GeV beam energy Q^2=9 GeV^2 is still practical in beam time. For a fixed Q^2 the Jacobian between the electron and proton solid angle changes with beam energy in such a way that if the electron solid angle is properly matched, the coincidence event rate is then largely independent of the beam energy. The smallest statistical error is then achieved at the energy for which the transverse polarization is maximum.

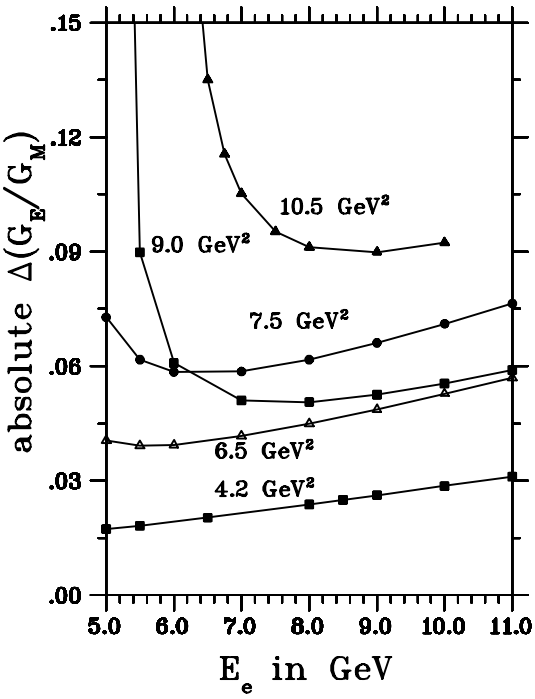

Figure 9: Predicted statistical uncertainties versus beam energy for the 3 new values of Q^2 proposed, and the control point at 4.2 GeV^2. Kinematic matching is assumed for each point. The curve at 10.5 GeV^2 demonstrates that for this Q^2 a beam energy of 7-8 GeV is required.

The kinematics of this proposal are listed in Table 1; the numbers are based on the following expectations:

• the beam helicity is h=0.8 and the current is 75 μA on the standard 15-cm long LH_2 cell (unpolarized hydrogen).

• The HMS solid angle is matched by the electron arm detector according to the Jacobian. This is achieved with a calorimeter consisting of an array of lead glass shower detectors. A calorimeter with active area of 2.56 m^2 will be located at various distances from the target to maintain kinematical matching. The minimum distance of 4.35 m occurs for Q^2=9 GeV^2.

• The HMS solid angle is 6 msr, and its angular resolution is 1-2 mr, both horizontally and vertically; these numbers take into account the use of an extended target.

• Estimates of the analyzing power and efficiency of the CH_2 analyzer used

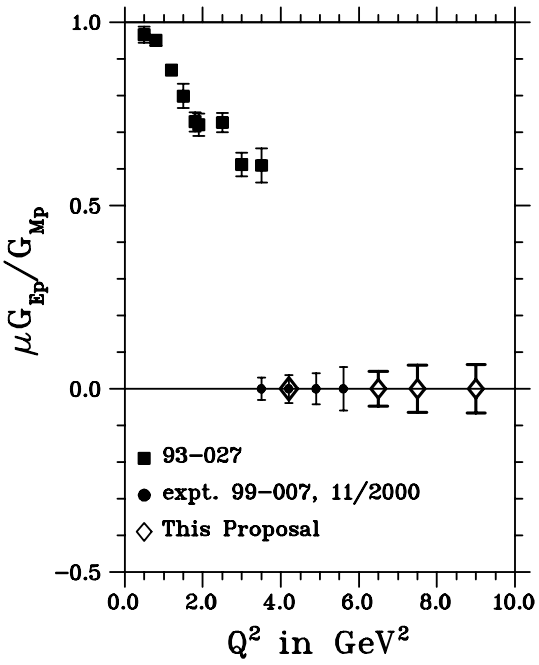

Figure 10: Predicted statistical error bars versus Q^2 for the 3 new values of Q^2 proposed, and the control point at 4.2 GeV^2. Kinematic matching is assumed for each point. The anticipated points are plotted arbitrarily at $\mu G_{Ep}/G_{Mp}$=0.

Q^2	E_e	θ_e	$E_{e'}$	θ_p	p_p	$d\sigma/d\Omega_e$	ϵA_y^2	χ	$\Delta\Omega_e$	rate
GeV^2	GeV	deg	GeV	deg	GeV/c	cm^2/sr	FOM	deg	msr	Hz
4.2	5.0	32	2.76	28	3.0	4.7×10^{-34}	0.01	152	8	117
6.5	6.0	38	2.5	21	4.3	3.8×10^{-35}	0.006	210	20	21
7.5	6.0	46	2.0	17	4.8	1.1×10^{-36}	0.005	236	37	12
9	6.0	68	1.2	11.4	5.66	1.4×10^{-37}	0.004	274	135	6

Table 1: Kinematics proposed.

to calculate rates and uncertainty, are made with a GEANT simulation[34].

• The analyzing power of the CH_2 does not need to be known to obtain the ratio G_{Ep}/G_{Mp}; however, the analyzing power will be measured simultaneously with G_{Ep}/G_{Mp}, for each of the 3 proton energies in this experiment(3.46, 4.00 and 4.78 GeV). For this calibration the beam polarization needs to be measured with the Hall C Møller polarimeter.

Q^2	E_e	absolute $\Delta(G_{Ep}/G_{Mp})$	time
GeV^2	GeV		hours
4.2	5.0	0.024	36
6.5	6.0	0.047	100
7.5	6.0	0.064	132
9	6.0	0.066	500
		TOTAL TIME	768

Table 2: Absolute uncertainties, including systematics, and times required. $\Delta(\mu G_{Ep}/G_{Mp})$ is the anticipated absolute uncertainty. Here we assume that $\mu G_{Ep}/G_{Mp}$ remains constant at 0.0, but in fact the absolute uncertainty $\Delta(\mu G_{Ep}/G_{Mp})$ is essentially independent of $\mu G_{Ep}/G_{Mp}$. A systematic uncertainty related to the precession angle is included per Equ.11.

when	what	goal	duration
2000-2001	lead-glass	background	2 shifts
2000-2001	HMS	background	1 shift
2003	calorimeter	install	1 month
2003	calorimeter	test	3 shifts
2004	polarimeter	install	1 month
2004	polarimeter	test	3 shifts

Table 3: Approximate times for pre-testing, assembling and final testing of components in Hall C

- The anticipated uncertainties shown in Table 2 and in Fig.10 for the 4 data points (4.2, 6.5, 7.5 and 9 GeV^2) are calculated from:

$$\frac{\Delta(G_{Ep}/G_{Mp)}}{G_{Ep}/G_{Mp}} = \sqrt{(\Delta a/a)^2 + (\Delta b/b)^2 + (\Delta \sin\chi/\sin\chi)^2}\ , \text{ where} \qquad (11)$$

$$\Delta a(\theta) = \Delta b(\theta) = \sqrt{\frac{2}{\epsilon(\theta) N_p(\theta)}} \qquad (12)$$

where a and b are the amplitudes in Equ.7, and N_p is the total number of protons entering the FPP.

This experiment will require time to measure the background in Hall C, to install the calorimeter and test it, and to install the FPP in the HMS and test it. Table 3 shows an outline of the approximate times required.

6 Conclusions

We propose to measure G_{Ep}/G_{Mp} to 9 GeV^2 in an experiment in Hall C, detecting the proton in the HMS and the electron in a large solid angle lead glass calorimeter. Such an experiment is possible before the anticipated energy upgrade shut down. The interest of continuing this experiment is obvious from the recently published results of experiment 93-027: the unexpected decrease of $\mu_p G_{Ep}/G_{Mp}$ from the dipole form factor value of 1 indicates that the charge and magnetic distributions in the proton are markedly different. The proposed experiment is an extension of experiment 99-007, which will measure G_{Ep}/G_{Mp} between 3.5 and 5.6 GeV^2 in steps of 0.7 GeV^2 at the end of this year (2000).

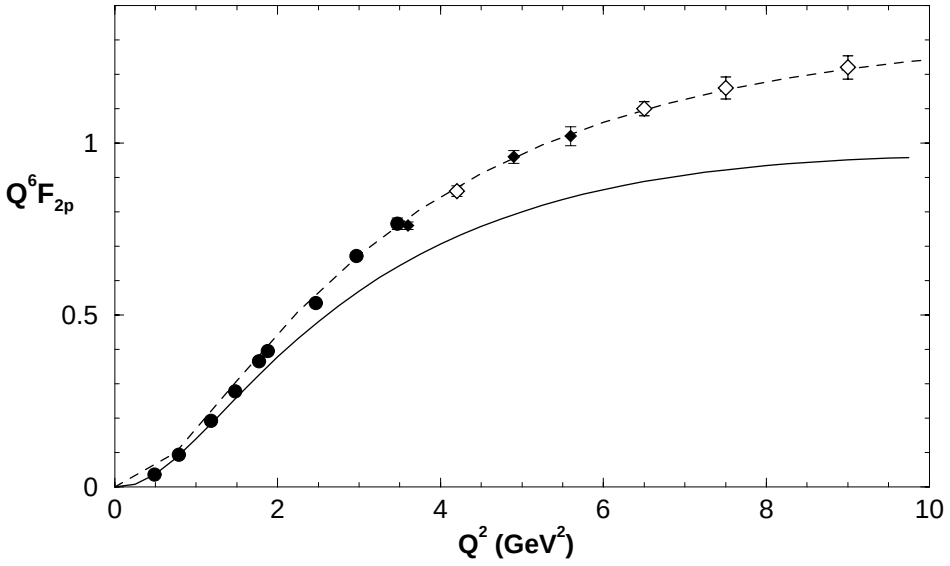

Figure 11: Same as Fig.4, with the anticipated uncertainties in this proposal (open circles), as well as the results of 93-027 (filled circles), showing them to be neither too large nor too small.

Previous form factor data have been interpreted in terms of an early onset of the perturbative QCD limit: $Q^2F_2/F_1 \sim constant$, as illustrated in Fig.2; the new data clearly demonstrate that this is not the case at such a low Q^2. The Q^2 region we will have explored when both 99-007 and this proposal are completed is potentially much more interesting: we could see a behavior similar to the one displayed by Q^4G_{Mp} or Q^4F_{1p}, around 9 GeV^2, or no such "asymptotic" behavior. In either case, characterizing F_{2p} to large Q^2 will shed light on the spin dependence of the quark-quark interaction at short distances. More generally, accurate measurements of hadronic form factors serve as a crucial test which theories must pass before they can be applied to other reactions such as meson photo- and electro-production, real Compton scattering, or deuteron photo-

disintegration.

The proposed measurement of G_{Ep}/G_{Mp} with small uncertainty and the existing cross section data[7, 9], together will bring the experimental characterization of G_{Ep} and G_{Mp} to equal levels of accuracy in this important regime. Likewise, the combination of the proposed data with the existing G_{Mp} data, will determine both F_{1p} and F_{2p} with small uncertainty. Therefore this experiment will extend the knowledge of F_{2p} to a Q^2 region where, in the pQCD picture, spin flip should become strongly suppressed, or equivalently, helicity conservation should operate. Fig.11 shows the expected uncertainties for Q^6F_{2p}. A continuation of these measurements to 9 GeV^2 is clearly of great interest. This Q^2 region is commonly believed to be the one of transition between soft and hard scattering, the most challenging theoretically. Ultimately, understanding of this difficult region will be achieved from QCD, the theory of strong interaction, and the data from this experiment will play an essential role toward this goal.

References

[1] M.K. Jones et al., Phys. Rev. Lett. 84, 1398 (2000).

[2] J. Litt *et al.*, Phys. Lett. B **31**, 40 (1970).

[3] Ch. Berger *et al.*, Phys. Lett. B **35**, 87 (1971).

[4] L.E. Price *et al.*, Phys. Rev. D **4**, 45 (1971).

[5] W. Bartel *et al.*, Nuc. Phys. B **58**, 429 (1973).

[6] R.C. Walker *et al.*, Phys. Rev. D **49**, 5671 (1994).

[7] L. Andivahis *et al.*, Phys. Rev. D **50**, 5491 (1994).

[8] B. Milbrath *et al.*, Phys. Rev. Lett. **80**, 452 (1998); erratum, Phys. Rev. Lett. **82**, 2221 (1999).

[9] A.F. Sill *et al.*, Phys. Rev. D **48**, 29 (1993). R. G. Arnold et al, P.R.L. 57 174 (1986).

[10] S.J. Brodsky and G.P. Lepage, Phys. Rev. D22, (1981) 2157.

[11] W.K. Brooks et al. CEBAF proposal 94-017.

[12] R. Madey et al. CEBAF proposal 93-038, and D.Day et al. CEBAF proposal 93-026.

[13] G. Höhler et al., Nucl. Phys. B **114**, (1976) 505.

[14] (a) M.F. Gari and W. Kruempelmann, Z. Phys. A322, (1985) 689; (b) M.F. Gari and W. Kruempelmann, Phys. Lett. B247 (1992) 159.

[15] P. Mergell, U.G. Meissner, D. Drechsler N.P. A596 (1996) 367 and A.W. Hammer, U.G. Meissner and D. Drechsel, P.L. B385 (1996) 343.

[16] P.L. Chung and F. Coester, Phys. Rev. D44, (1991) 229.

[17] I. G. Aznauryan, Phys. Lett. B 316, (1993) 391.

[18] M.R. Frank, B.K. Jennings and G.A. Miller, Phys. Rev. C54 (1996) 920.

[19] P. Kroll, M. Schurmann and W. Schweiger, Z. Phys. A - Hadrons and Nuclei 338, (1991) 339.

[20] A.V. Radyushkin, Acta Phys. Polnica B 15, (1984) 40.

[21] D.H. Lu, A.W. Thomas and A.G. Williams, Phys. Rev. 57 (1998) 2628.

[22] P. E. Bosted, Phys. Rev. C51, (1995) 409.

[23] S.M. Bilenky, C. Giunti and V. Wataghin, hep-ph/9304221.

[24] V.A. Nesterenko and A.V. Radyushkin, Phys. Lett. 115B (1982) 410.

[25] N. Isgur and C.H. Llewellyn Smiths, Phys. Rev. Lett. 52 (1984) 1080.

[26] X. Ji, Phys. Rev. D55 (1997) 7114, Phys. Rev. Lett. 78 (1997) 610.

[27] A.V. Radyushkin JLab-THY-98-10 and hep-ph/9803316 v2.

[28] A.V. Afanasev hep-ph/9808291 v2.

[29] A.V. Afanasev, private communication, 1999 and contribution to the "Exclusive and Semi-exclusive Processes at High Momentum Transfer, JLab 5/99.

[30] J. Ashman et al., Phys. Lett. 206B, 364 (1988); D. Adams et al., Phys. Rev. D56, 5330 (1997); K. Abe et al., Phys. Rev. D58, 112003 (1998)

[31] N. Mathur, S.J. Dong, K.F. Liu, L. Mankiewicz and N.C. Mukhopadhyay, hep-ph/9912289

[32] A.I. Akhiezer and M.P. Rekalo, Sov. J. Part. Nucl. **3**, 277 (1974).

[33] R. Arnold, C. Carlson and F. Gross, Phys. Rev. C **23**, 363 (1981).

[34] A. Fleck and E.J. Brash internal report April 20, 1999.

[35] E.V. Anoshina et al., Phys. of Atomic Nuclei, 60 (1997) 224.

[36] D. Miller et al. Phys. Rev. D 16, 2016 (1977) and Diebold et al. P.R.L. 35, 632 (1975); both data cover the energy of this proposal.

[37] JLab approved experiment 97-108 B. Wojtsekhowsky, C. Hyde-Wright and A. Nathan.